arXiv:1611.08772v1 [math.NA] 27 Nov 2016

SUBSTRUCTURING PRECONDITIONERS WITH NOVEL INTERFACE SOLVERS FOR GENERAL ELLIPTIC-TYPE EQUATIONS IN THREE DIMENSIONS

QIYA HU AND SHAOLIANG HU

Abstract. In this paper we propose two variants of the substructuring preconditioner for solving three-dimensional elliptic-type equations with strongly discontinuous coefficients. In the new preconditioners, we use the simplest coarse solver associated with the finite element space induced by the coarse partition, and construct novel interface solvers based on some new observations. The resulting preconditioners share the merits of the non-overlapping domain decomposition method (DDM) and the overlapping DDM in the sense that they not only are cheap but also are easy to implement. We apply the proposed preconditioners to solve the linear elasticity problems and Maxwell's equations in three dimensions. Numerical results show that the convergence rate of PCG method with the preconditioners are nearly optimal, and also robust with respect to the (possibly large) jumps of the coefficients in the considered equations.

Keywords: domain decomposition, substructuring preconditioner, linear elasticity problems, Maxwell's equations, PCG iteration, convergence rate

AMS subject classifications. 65N30, 65N55.

1. Introduction

There are many works to study (non-overlapping or overlapping) domain decomposition methods (DDMs) for solving the systems generated by finite element discretization of elliptic-type partial differential equations ([1]-[5],[7]-[24], [26], [28]-[39], [41]-[43], [45]-[46],[44, 48] and the references therein). Non-overlapping DDMs and overlapping DDMs have their respective merits and drawbacks: non-overlapping DDMs are cheaper and more efficient for the case of large jump coefficient than overlapping DDMs (with large overlap), but non-overlapping DDMs are more difficult to construct and implement than overlapping DDMs. In fact, the construction of non-overlapping DDMs heavily depends on the considered models. For example, non-overlapping DDMs for positive definite Maxwell's equations are essentially different from that for the usual elliptic equation (comparing [13, 31, 33, 43]). The drawbacks mentioned above restrict applications of the non-overlapping DDMs

LSEC, Institute of Computational Mathematics and Scientific Engineering Computing, Chinese Academy of Sciences, Beijing 100080, China (hqy@lsec.cc.ac.cn) and hushaoliang@lsec.cc.ac.cn).
This work was funded by Natural Science Foundation of China G11571352.

and the overlapping DDMs with large overlap. Although the overlapping DDMs with small overlap are cheap and easy to implement, they have slower convergence. Over the past two decades, some interesting DDMs have been proposed and analyzed, for example, the DDMs with Lagrangian multipliers [19, 20, 30, 34] , the BDDC methods [11, 13, 36, 38], the restricted additive Schwarz methods [5, 22], the optimized Schwarz methods [23, 24]. These methods have obvious advantages over the traditional DDMs: the DDMs with Lagrangian multipliers can be conveniently handle non-matching grids, the BDDC methods are particularly practical for the case with irregular subdomains, the restricted additive Schwarz methods are cheaper and faster than the standard overlapping DDMs, the optimized Schwarz methods can accelerate convergence of the non-overlapping Schwarz methods.

In the present paper, we try to construct relatively united substructuring preconditioners for elliptic-type equations, such that they are cheap, easy to implement and have fast convergence. As usual, we decompose the considered domain into the union of some non-overlapping subdomains, which constitute a coarse partition of the domain. In the proposed preconditioners, we use the simplest coarse space induced by the coarse partition as in the overlapping DDMs. The main goal of this paper is to design cheap and practical local interface solvers based on some new observations.

For each internal cross-point, we introduce an auxiliary subdomain that contains the internal cross-point as its "center" and has almost the same size with the original subdomains. Associated with each auxiliary subdomain, we define a local interface problem such that the solution of the local interface problem is discrete harmonic in the intersection of the auxiliary subdomain with every original subdomain adjoining it. Notice that each intersection is only a part of some original subdomain, so the local interface problem is defined on a space consisting of "inexact" harmonic extensions. The corresponding local interface solver is implemented by solving a Dirichlet problem (residual equation), which is defined on the natural restriction space of the original finite element space on the auxiliary subdomain. It is clear that each local interface solver has almost the same cost with an original subdomain solver. We would like to point out that the proposed local interface solvers are different from the existing local interface solvers defined in the vertex space method [41] or the interface overlapping additive Schwarz [48], where exact harmonic extensions are required.

In order to further reduce the cost of the local interface solvers described above, we need to decompose each local interface problem into two subproblems and present approximate local interface solvers based on a coarsening technique. In the step for solving a local interface problem, we are interested only in the degrees of freedom on the local interface, instead of the degrees of freedom in the interiors of subdomains. Intuitively, the accuracy of the degrees of freedom on the local

interface are not sensitive to the grids far from the local interface. Based on this observation, we construct auxiliary non-uniform grids in each subdomain adjoining the considered local interface such that the auxiliary grids coincide with the original fine grids on the local interface but gradually become coarser when nodes are far from the local interface. These auxiliary grids can be easily generated by the existing software and contain much smaller number of nodes than the original fine grids in a subdomain. Such an approximate local interface solver is implemented by solving a Dirichlet problem on the finite element space defined by the auxiliary grids, and so it is much cheaper than the original local interface solver.

The constructions of the coarse solver and the proposed local interface solvers do not depend on the considered models, and the resulting substructuring preconditioners are cheap and easy to implement. As pointed out in [13], the design of an efficient substructuring preconditioner for three dimensional Maxwell's equations poses quite significant challenges. A few existing preconditioners on this topic are either expensive or difficult to implement. We will apply the proposed substructuring preconditioners to solve the linear elasticity problems and Maxwell's equations in three dimensions. Numerical results show that the preconditioners are robust uniformly for the two kinds of equations even if the coefficients have large jumps.

The outline of the paper is as follows. In Section 2, we give the variational formula of general elliptic-type equations and introduce a partition based on domain decomposition. In Section 3, we describe local interface solvers associated with vertex-related subdomains and define the resulting substructuring preconditioner for the general elliptic system. In Section 4, we design cheaper local interface solvers and present the corresponding preconditioner based on a coarsening technique. In Section 5, we discuss applications of the substructuring methods to elasticity problems and Maxwell's equations. In section 6, we will report some numerical results for the linear elasticity problems and Maxwell's equations.

2. Elliptic-type equations and domain decomposition

In this section, we describe the considered problems.

2.1. **Elliptic-type equations.** Let Ω be a bounded and connected Lipschitz domain in $\mathbb{R}^3$. For convenience, we just consider the weak form of elliptic-type equations. Let $V(\Omega)$ denote a Hilbert space with the scalar product $(\cdot,\cdot)_V$, and $||\cdot||_V$ be the induced norm. We introduce a real bilinear form $\boldsymbol{\mathcal{A}}(\cdot,\cdot) : V(\Omega)\times V(\Omega) \to R$. We assume that $\boldsymbol{\mathcal{A}}(\cdot,\cdot)$ is symmetric, continuous and coercive in the sense that

$$\boldsymbol{\mathcal{A}}(\mathbf{u},\mathbf{v}) = \boldsymbol{\mathcal{A}}(\mathbf{v},\mathbf{u}), \quad |\boldsymbol{\mathcal{A}}(\mathbf{u},\mathbf{v})| \le c_1||\mathbf{u}||_V||\mathbf{v}||_V, \quad \forall \mathbf{u},\mathbf{v} \in V(\Omega)$$

and

$$\boldsymbol{\mathcal{A}}(\mathbf{u},\mathbf{u}) \ge c_2||\mathbf{u}||_V^2, \quad \forall \mathbf{u} \in V(\Omega)$$

for two positive number c_1 and c_2.

Given a linear functional $\boldsymbol{F} \in V'(\Omega)$, we consider the following problem:

$$\begin{cases} Find \quad \mathbf{u} \in V(\Omega) \quad .st. \\ \boldsymbol{\mathcal{A}}(\mathbf{u}, \mathbf{v}) = \langle \boldsymbol{F}, \mathbf{v} \rangle, \quad \forall \mathbf{v} \ \in V(\Omega) \end{cases} \tag{2.1}$$

2.2. **Domain decomposition and discretization.** For convenience, we assume that Ω is a polyhedra. For a number $d \in (0,\ 1)$, let Ω be decomposed into the union of non-overlapping tetrahedra (or hexahedra) $\{\Omega_k\}$ with the size d. Then we get a non-overlapping domain decomposition for Ω: $\bar{\Omega} = \bigcup_{k=1}^{N} \bar{\Omega}_k$. Assume that $\Omega_i \cap \Omega_j = \emptyset$ when $i \neq j$; if $i \neq j$ and $\partial\Omega_i \cap \partial\Omega_j \neq \emptyset$, then $\partial\Omega_i \cap \partial\Omega_j$ is a common, or a common edge, or a common vertex of Ω_i and Ω_j. It is clear that the subdomains $\Omega_1, \cdots, \Omega_N$ constitute a *coarse* partition $\mathcal{T}_d$ of Ω. If $\partial\Omega_i \cap \partial\Omega_j$ is just a common face of Ω_i and Ω_j, then set $\Gamma_{ij} = \partial\Omega_i \cap \partial\Omega_j$. Define $\Gamma = \cup\Gamma_{ij}$. By Γ_k we denote the intersection of Γ with the boundary of the subdomain Ω_k. So we have $\Gamma_k = \partial\Omega_k$ if Ω_k is an interior subdomain of Ω.

With each subdomain Ω_k we associate a regular partition made of tetrahedral elements (or hexahedral elements). We require that the partitions in all the subdomains match on the common face between two neighboring subdomains, and so they constitute a partition $\mathcal{T}_h$ on the domain Ω, which we assume is quasi-uniform. We denote by h the mesh size of $\mathcal{T}_h$, i.e., h denotes the maximum diameter of tetrahedra in the mesh $\mathcal{T}_h$.

For an element $K \in \mathcal{T}_h$, let $R(K)$ denote a set of basis functions on the element K. The definition of $R(K)$ depends on the considered models, and will be given in Section 5. Define the finite element space

$$V_h(\Omega) = \Big\{ \mathbf{v} \in V(\Omega) :\ \mathbf{v}|_K \in R(K),\ \forall K \in \mathcal{T}_h \Big\}.$$

Consider the discrete problem of (2.1): *Find* $\boldsymbol{u}_h \in V_h(\Omega)$ *such that*

$$\boldsymbol{\mathcal{A}}(\boldsymbol{u}_h, \boldsymbol{v}) = \langle \boldsymbol{F}, \boldsymbol{v} \rangle, \quad \forall \boldsymbol{v} \in V_h(\Omega). \tag{2.2}$$

This is the discrete variational problem that we need to solve in this paper.

For convenience, we define the discrete operator $A : V_h(\Omega) \to V_h(\Omega)$ as

$$\langle A\mathbf{u}, \mathbf{v} \rangle = \boldsymbol{\mathcal{A}}(\mathbf{u}, \mathbf{v}), \quad \mathbf{u}, \mathbf{v} \in V_h(\Omega),$$

where $\langle \cdot, \cdot \rangle$ denotes the duality pairing between $V'(\Omega)$ and $V(\Omega)$. Then (2.2) can be written in the operator form

$$Au_h = \boldsymbol{f}. \tag{2.3}$$

By the assumptions on $\mathcal{A}(\cdot, \cdot)$, the operator is symmetric and positive definite. Thus the above equation can be iteratively solved by PCG method. In the rest of this paper, we will construct preconditioners for the operator A.

Before constructing the desired preconditioners, we first introduce some useful sets and subspaces.

$\mathcal{N}_h$: the set of all nodes generated by the *fine* partition $\mathcal{T}_h$;
$\mathcal{E}_h$: the set of all *fine* edges generated by the partition $\mathcal{T}_h$;
$\mathcal{F}_h$: the set of all *fine* faces generated by the partition $\mathcal{T}_h$;
$\mathcal{N}_d$: the set of all nodes generated by the *coarse* partition $\mathcal{T}_d$.

In most applications, the degrees of freedom of $\mathbf{v} \in V_h(\Omega)$ are defined at the nodes in $\mathcal{N}_h$ (the nodal elements), or on the edges in $\mathcal{E}_h$ (Nedelec edge elements), or on the faces in $\mathcal{F}_h$ (Raviart-Thomas face elements). Throughout this paper, for a subset F that is the union of faces in $\mathcal{F}_h$, the term "the degrees of freedom of $\mathbf{v}$ vanish on F" means that "$\mathbf{v}$ has the zero degrees of freedom at the nodes, or fine edges, or fine faces of F".

Let $G \subset \Omega$ be a subdomain that is the union of some elements in $\mathcal{T}_h$. Define

$$V_h^0(G) = \{v \in V_h(\Omega) : \text{ the degrees of freedom of } \mathbf{v} \text{ vanish on } \partial G\}.$$

For example, when $G = \Omega_k$ the space $V_h^0(\Omega_k)$ is just the subdomain space in the traditional substructuring methods.

For the construction of preconditioners, we will use the simplest coarse space $V_d(\Omega)$, which is defined as the finite element space associated with the *coarse* partition $\mathcal{T}_d$ (see [15], [30], [31] and [48]). It is clear that $V_d(\Omega) \subset V_h(\Omega)$.

3. Preconditioner (I): with local interface solvers related to vertices

This section is devoted to describing the first preconditioner, in which local interface solvers are defined in vertex-related subspaces.

3.1. **Space decomposition.** For each V $\in \mathcal{N}_d$, we construct an open region $\Omega_{\rm V}^{half}$, whose "center" is V and size is about d. When V $\in \partial\Omega$, the auxiliary subdomain $\Omega_{\rm V}^{half}$ is chosen as the part in Ω. We assume that: (i) each subdomain $\Omega_{\rm V}^{half}$ is just the union of some elements in $\mathcal{T}_h$; (ii) the union of all the subdomains $\Omega_{\rm V}^{half}$ is an open cover of Ω. Then all the subdomains $\Omega_{\rm V}^{half}$ constitute overlapping domain decomposition of Ω (with small overlap).

In order to define a space decomposition of $V_h(\Omega)$ in an exact manner, we need to introduce more notations.

For V $\in \mathcal{N}_d$, set

$$\Lambda_{\rm V} = \{k : \text{ the polyhedran } \Omega_k \text{ contains V as its vertex}\}$$

and define

$$\Gamma_{\rm V}^{half} = \Omega_{\rm V}^{half} \cap \Gamma \text{ and } \Omega_{\rm V} = \bigcup_{k \in \Lambda_{\rm V}} \Omega_k.$$

Let $V_h(\Gamma)$ denote the interface space, which consists of the natural traces of all the functions in $V_h(\Omega)$. Define the vertex-related local interface space

$$V_h^0(\Gamma_{\rm V}^{half}) = \{\phi \in V_h(\Gamma) : \ supp\ \phi \subset \Gamma_{\rm V}^{half}\}.$$

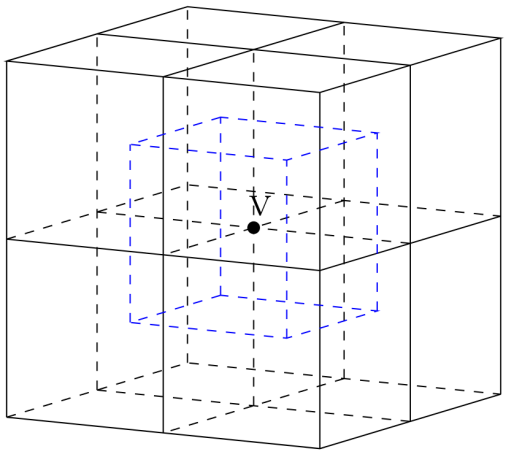

FIGURE 1. The auxiliary subdomain $\Omega_{\mathrm{V}}^{half}$ (the blue cube) associated with the vertex V.

Since all the vertex-related local interfaces $\Gamma_{\mathrm{V}}^{half}$ constitute an open cover of the interface Γ, we have the space decomposition

$$V_h(\Gamma) = \bigcup_{\mathrm{V}\in\mathcal{N}_d} V_h^0(\Gamma_{\mathrm{V}}^{half}). \tag{3.1}$$

As usual, let $V_h^{\perp}(\Omega)$ denote the space consisting of all the finite element functions that are discrete A-harmonic in each Ω_k, namely

$$V_h^{\perp}(\Omega) = \{\mathbf{v} \in V_h(\Omega) :\ \mathcal{A}(\mathbf{v}, \mathbf{w}) = 0,\ \forall \mathbf{w} \in V_h^0(\Omega_k)\ \textit{for each}\ k \in \mathcal{N}_d\}.$$

Then we have

$$V_h(\Omega) = V_d(\Omega) + \sum_{k=1}^{N} V_h^0(\Omega_k) + V_h^{\perp}(\Omega). \tag{3.2}$$

For each $\mathrm{v} \in \mathcal{N}_d$, define vertex-related local A-harmonic space

$$V_h^{\perp}(\Omega_{\mathrm{V}}) = \{\mathbf{v} \in V_h^{\perp}(\Omega) :\ \text{the trace of } \mathbf{v} \text{ belongs to } V_h^0(\Gamma_{\mathrm{V}}^{half})\} \subset V_h^0(\Omega_{\mathrm{V}}).$$

In other words, $V_h^{\perp}(\Omega_{\mathrm{V}})$ is just the space consisting of the discrete A-harmonic extensions of the functions in $V_h^0(\Gamma_{\mathrm{V}}^{half})$.

It is clear that

$$V_h^{\perp}(\Omega) = \bigcup_{\mathrm{V}\in\mathcal{N}_d} V_h^{\perp}(\Omega_{\mathrm{V}}).$$

Thus, by (3.2), the space $V_h(\Omega)$ admits the space decomposition

$$V_h(\Omega) = V_d(\Omega) + \sum_{k=1}^{N} V_h^0(\Omega_k) + \sum_{\mathrm{V}\in\mathcal{N}_d} V_h^{\perp}(\Omega_{\mathrm{V}}). \tag{3.3}$$

3.2. **Preconditioner.** In this subsection we define solvers on the subspaces $V_d(\Omega)$, $V_h^0(\Omega_k)$ and $V_h^\perp(\Omega_{\rm V})$.

As usual, we use $A_d : V_d(\Omega) \to V_d(\Omega)$ and $A_k : V_h^0(\Omega_k) \to V_h^0(\Omega_k)$ to denote the restriction of A on $V_d(\Omega)$ and $V_h^0(\Omega_k)$ respectively, i.e., they satisfy

$$(A_d\mathbf{v}_d, \mathbf{w}_d) = (A\mathbf{v}_d, \mathbf{w}_d) = \boldsymbol{\mathcal{A}}(\mathbf{v}_d, \mathbf{w}_d),\ \mathbf{v}_d \in V_d(\Omega),\ \forall \mathbf{w} \in V_d(\Omega)$$

and

$$(A_k\mathbf{v}, \mathbf{w})_{\Omega_k} = (A\mathbf{v}, \mathbf{w}) = \boldsymbol{\mathcal{A}}(\mathbf{v}, \mathbf{w}),\ \mathbf{v} \in V_h^0(\Omega_k),\ \forall \mathbf{w} \in V_h^0(\Omega_k).$$

In the following we define an "inexact" solver on $V_h^\perp(\Omega_{\rm V})$. To this end, we introduce a modification of $V_h^\perp(\Omega_{\rm V})$. Let $k \in \Lambda_{\rm V}$, and use $\Omega_{{\rm V},k}^{half}$ to denote the intersection of $\Omega_{\rm V}^{half}$ with Ω_k. For each $\Omega_{\rm V}^{half}$, define the "inexact" A-harmonic space

$$V_h^\perp(\Omega_{\rm V}^{half}) = \{\mathbf{v} \in V_h^0(\Omega_{\rm V}^{half}) :\ \mathcal{A}(\mathbf{v}, \mathbf{w}) = 0,\ \forall \mathbf{w} \in V_h^0(\Omega_{{\rm V},k}^{half}) \text{ with } k \in \Lambda_{\rm V}\}.$$

Notice that the functions in $V_h^\perp(\Omega_{\rm V}^{half})$ have the support set $\Omega_{\rm V}^{half}$ and are discrete A-harmonic only in the subdomain $\Omega_{{\rm V},k}^{half}$ of Ω_k (for any $k \in \Lambda_{\rm V}$). Thus the spaces $V_h^\perp(\Omega_{\rm V}^{half})$ have essential differences from the local interface spaces proposed in the vertex space method [41] or the interface overlapping additive Schwarz [48], where exact A-harmonic extensions in all Ω_k were required.

For a function $\mathbf{v} \in V_h^\perp(\Omega_{\rm V})$, define $\mathbf{v}^{half} \in V_h^\perp(\Omega_{\rm V}^{half})$ such that $\mathbf{v}^{half} = \mathbf{v}$ on $\Gamma_{\rm V}^{half}$. For each ${\rm v} \in \mathcal{N}_d$, let $B_{\rm V} : V_h^\perp(\Omega_{\rm V}) \to V_h^\perp(\Omega_{\rm V})$ be the symmetric and positive definite operators defined by

$$(B_{\rm V}\mathbf{v}, \mathbf{w}) = \boldsymbol{\mathcal{A}}(\mathbf{v}^{half}, \mathbf{w}^{half}), \quad \mathbf{v} \in V_h^\perp(\Omega_{\rm V}),\ \forall \mathbf{w} \in V_h^\perp(\Omega_{\rm V}).$$

Since the basis functions in $V_h^\perp(\Omega_{\rm V})$ are not known, the action of $B_{\rm V}^{-1}$ needs to be implemented by solving a residual equation defined in $V_h^0(\Omega_{\rm V}^{half})$ (see **Algorithm 3.1** given later).

Let $Q_d : V_h(\Omega) \to V_d(\Omega)$, $Q_k : V_h(\Omega) \to V_h^0(\Omega_k)$ and $Q_{\rm V} : V_h(\Omega) \to V_h^\perp(\Omega_{\rm V})$ be the standard L^2-projectors. Then the first preconditioner for A is defined as follows:

$$B_I^{-1} = A_d^{-1}Q_d + \sum_{k=1}^{N} A_k^{-1}Q_k + \sum_{{\rm V}\in\mathcal{N}_d} B_{\rm V}^{-1}Q_{\rm V} \tag{3.4}$$

Remark 3.1. *To our knowledge, the coarse solver A_d is the simplest and cheapest one in the non-overlapping DDMs. This coarse solver for elliptic equation was first considered in* [15]*, and then discussed in* [48]*. Such coarse solver was regarded as a non-optional coarse solver for long time, since the condition number of the resulting preconditioned system is not nearly optimal for the case with large jump coefficients. Based on the framework developed in* [47]*, it was shown in* [30] *that the PCG method for solving the resulting preconditioned system has the nearly stable convergence even for the case with large jump coefficients. In* [31]*, this kind of coarse solver was also applied to Maxwell's equations. When this coarse solver are used,*

cheap "edge" solvers (and "face" solvers) need to be designed. It can be seen, from [31] *and* [30] *(see also* [15] *and* [48]*), that the constructions of the existing "edge" solvers are based on estimates of the norms induced from the interface operators restricted on the edges and so depend on the considered models. In the proposed preconditioner B_I, the construction of the edge solvers $B_{\rm V}$ (which also play the role of face solvers) is unified and independent of the bilinear $\boldsymbol{\mathcal{A}}(\cdot,\cdot)$.*

Remark 3.2. *The preconditioner (3.4) can be extended to the case with irregular subdomains (i.e., Ω_k is not a polyhedron with finite faces), for which the coarse space $V_d(\Omega)$ needs to be replaced by the image of the interpolation operator from an auxiliary regular coarse space into $V_h(\Omega)$ as in* [4] *and* [7].

The action of the preconditioner B_I^{-1}, which is needed in each iteration step of PCG method, can be described by the following algorithm.

Algorithm 3.1. For $\mathbf{g}\in V_h(\Omega)$, we can compute $\mathbf{u}=B_I^{-1}\mathbf{g}$ in four steps.

Step 1. Solve the system of $\mathbf{u}_d\in V_d(\Omega)$:

$$(A_d\mathbf{u}_d,\mathbf{v}_d)=(\mathbf{g},\mathbf{v}_d),\ \forall\mathbf{v}_d\in V_d(\Omega);$$

Step 2. Solve the systems of $\mathbf{u}_k\in V_h^0(\Omega_k)$ $(k=1,\cdots,N)$ in parallel:

$$(A_k\mathbf{u}_k,\mathbf{v})=(\mathbf{g},\mathbf{v}),\ \forall\mathbf{v}\in V_h^0(\Omega_k),\ k=1,\cdots,N;$$

Step 3. Solve the systems of $\mathbf{u}_{\rm V}\in V_h^0(\Omega_{\rm V}^{half})$ $({\rm V}\in\mathcal{N}_d)$ in parallel:

$$(B_{\rm V}\mathbf{u}_{\rm V},\mathbf{v})=(\mathbf{g},\mathbf{v})-\sum_{k\in\Lambda_{\rm V}}(A_k\mathbf{u}_k,\mathbf{v})_{\Omega_k},\ \forall\mathbf{v}\in V_h^0(\Omega_{\rm V}^{half});$$

Step 4. Compute the trace $\Phi_h=\boldsymbol{\gamma}_\Gamma(\sum\limits_{{\rm V}\in\mathcal{N}_d}\mathbf{u}_{\rm V})$, and then compute the A-harmonic extension of Φ_h on each Ω_k to obtain $\mathbf{u}^\perp\in V_h^\perp(\Omega)$. This leads to

$$\mathbf{u}=\mathbf{u}_d+\sum_{k=1}^N\mathbf{u}_k+\mathbf{u}^\perp.$$

Remark 3.3. *It can be seen from* **Algorithm 3.1** *that the preconditioner (3.4) is easy and cheap to implement (each vertex-related space $V_h^0(\Omega_{\rm V}^{half})$ has almost the same degrees of freedom with an original subdomain space $V_h^0(\Omega_k)$).*

4. Preconditioner (II): with approximate interface solvers

Although the local interface solvers $B_{\rm V}$ defined in the last section is not expensive, we want to further reduce the cost for implementing the action of $B_{\rm V}^{-1}$. To this end, we introduce a coarsening technique for the construction of cheaper local interface solvers.

$\mathcal{F}_d$: the set of all the open (coarse) faces generated by the partition $\mathcal{T}_d$;

$\mathcal{E}_d$: the set of all the open (coarse) edges generated by the partition $\mathcal{T}_d$;

$\mathcal{F}_{\rm V}$: the set of the (coarse) faces, each of which belongs to $\mathcal{F}_d$ and contains V as its vertex;

$\mathcal{E}_{\rm V}$: the set of the (coarse) edges, each of which belongs to $\mathcal{E}_d$ and contains V as its vertex;

For $\mathrm{E} \in \mathcal{E}_{\rm V}$, let $W_{\rm E} \subset \Gamma$ denote the union of the face support sets of the basis functions associated with the fine grids on E. Define

$$W_{\rm V}^{half} = \big(\bigcup_{\mathrm{E}\in\mathcal{E}_{\rm V}} W_{\rm E}\big) \bigcap \Gamma_{\rm V}^{half}.$$

Namely, $W_{\rm V}^{half}$ is the intersection of $\Gamma_{\rm V}^{half}$ with the union of the face fine elements adjoining $\mathrm{E} \in \mathcal{E}_{\rm V}$. Although the set $W_{\rm V}^{half}$ looks like the *wire-basket* set in the BPS substructuring method, they have some differences: $W_{\rm V}^{half}$ is a vertex-related set, but the *wire-basket* set is subdomain-related; the *wire-basket* set has zero measure in Γ, but the set $W_{\rm V}^{half}$ does not.

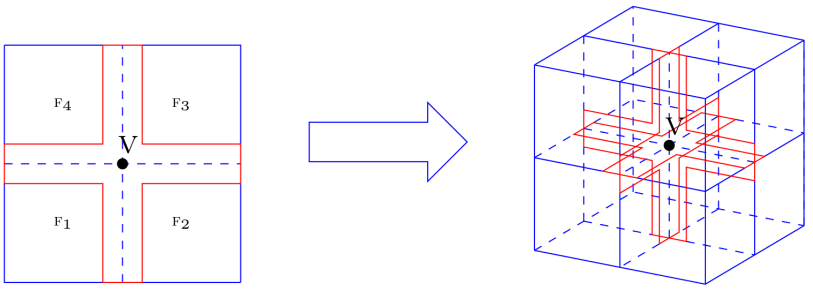

(a) 2D cross section (b) 3D $W_{\rm V}^{half}$ and $\Omega_{\rm V}^{half}$

FIGURE 2. the structure of $W_{\rm V}^{half}$ (red) in $\Omega_{\rm V}^{half}$ (blue)

Set

$$F_{\rm V}^{in} = \Gamma_{\rm V}^{half} \backslash W_{\rm V}^{half},$$

in other words, $F_{\rm V}^{in}$ is the intersection of $\Gamma_{\rm V}^{half}$ with the union of the fine elements on the interior of the faces in $\mathcal{F}_{\rm V}$. Define

$$\hat{V}_h^0(\Gamma_{\rm V}^{half}) = \{\mathbf{v} \in V_h^0(\Gamma_{\rm V}^{half}) : \text{ the degrees of freedom of } \mathbf{v} \text{ vanish on } F_{\rm V}^{in}\}.$$

Namely, the space $\hat{V}_h^0(\Gamma_{\rm V}^{half})$ keeps the "edge" degrees of freedom of $V_h^0(\Gamma_{\rm V}^{half})$ but drops the "face" degrees of freedom. For each $\mathrm{F} \in \mathcal{F}_d$, define the local interface space

$$V_h^0(\mathrm{F}) = \{\phi \in V_h(\Gamma) : \ supp\ \phi \subset \mathrm{F}\}.$$

It is clear that

$$V_h^0(\Gamma_{\rm V}^{half}) = \hat{V}_h^0(\Gamma_{\rm V}^{half}) + \big(\sum_{\mathrm{F}\in\mathcal{F}_{\rm V}} V_h^0(\mathrm{F})\big) \cap V_h^0(\Gamma_{\rm V}^{half}). \tag{4.1}$$

Thus, by (3.1) we have the space decomposition

$$V_h(\Gamma) = \sum_{\mathrm{V}\in\mathcal{N}_d} \hat{V}_h^0(\Gamma_{\mathrm{V}}^{half}) + \sum_{\mathrm{F}\in\mathcal{F}_d} V_h^0(\mathrm{F}). \tag{4.2}$$

Let Ω_{F} be the union of F itself and the two subdomains that have F as their common face. Define

$$\hat{V}_h^{\perp}(\Omega_{\mathrm{V}}) = \{\mathbf{v} \in V_h^{\perp}(\Omega_{\mathrm{V}}) : \text{ the trace of } \mathbf{v} \text{ belongs to } \hat{V}_h^0(\Gamma_{\mathrm{V}}^{half})\} \ (\mathrm{V} \in \mathcal{N}_d)$$

and

$$V_h^{\perp}(\Omega_{\mathrm{F}}) = \{\mathbf{v} \in V_h^{\perp}(\Omega) : \text{ the trace of } \mathbf{v} \text{ belongs to } V_h^0(\mathrm{F})\} \ (\mathrm{F} \in \mathcal{F}_d).$$

Namely, $\hat{V}_h^{\perp}(\Omega_{\mathrm{V}})$ and $V_h^{\perp}(\Omega_{\mathrm{F}})$ consist of the A-harmonic extensions of the functions in $\hat{V}_h^0(\Gamma_{\mathrm{V}}^{half})$ and $V_h^0(\mathrm{F})$, respectively. Corresponding to (4.2), we have

$$V_h^{\perp}(\Omega) = \sum_{\mathrm{V}\in\mathcal{N}_d} \hat{V}_h^{\perp}(\Omega_{\mathrm{V}}) + \sum_{\mathrm{F}\in\mathcal{F}_d} V_h^{\perp}(\Omega_{\mathrm{F}}).$$

Thus, by (3.2), we obtain another space decomposition

$$V_h(\Omega) = V_d(\Omega) + \sum_{k=1}^{N} V_h^0(\Omega_k) + \sum_{\mathrm{V}\in\mathcal{N}_d} \hat{V}_h^{\perp}(\Omega_{\mathrm{V}}) + \sum_{\mathrm{F}\in\mathcal{F}_d} V_h^{\perp}(\Omega_{\mathrm{F}}). \tag{4.3}$$

The space decomposition (4.3) seems more complicated than the space decomposition (3.3), but each subspace in the second sum and the third sum of (4.3) has different structure from $V_h^{\perp}(\Omega_{\mathrm{V}})$, which can help us to construct cheaper local interface solvers in the next subsection.

4.1. **Approximate local interface solvers.** For $\mathrm{F} \in \mathcal{F}_d$, define the operator A_{F} as the restriction of A on the subspace $V_h^{\perp}(\Omega_{\mathrm{F}})$, i.e., it satisfies

$$(A_{\mathrm{F}}\mathbf{v}, \mathbf{w}) = \mathcal{A}(\mathbf{v}, \mathbf{w}), \ \mathbf{v} \in V_h^{\perp}(\Omega_{\mathrm{F}}), \ \forall \mathbf{w} \in V_h^{\perp}(\Omega_{\mathrm{F}}).$$

As usual, the action of A_{F}^{-1} can be implemented by solving the following residual equation: to find $\mathbf{u}_{\mathrm{F}} \in V_h^0(\Omega_{\mathrm{F}})$ such that

$$\mathcal{A}(\mathbf{u}_{\mathrm{F}}, \mathbf{w}) = (\mathbf{g}, \mathbf{w}) - \sum_{k\in\Lambda_{\mathrm{F}}} \mathcal{A}(\mathbf{u}_k, \mathbf{w}), \ \forall \mathbf{w} \in V_h^0(\Omega_{\mathrm{F}}), \tag{4.4}$$

where $\mathbf{g} \in V_h(\Omega)$ is given, and $\mathbf{u}_k \in V_h^0(\Omega_k)$ has been gotten by solving the local equation

$$\mathcal{A}(\mathbf{u}_k, \mathbf{w}) = (\mathbf{g}, \mathbf{w}), \ \forall \mathbf{w} \in V_h^0(\Omega_k).$$

But, the calculation of $\mathbf{u}_{\mathrm{F}}$ is expensive, so we propose a new way to compute a rough approximation of $\mathbf{u}_{\mathrm{F}}$ in the following.

Let Ω_1^{F} and Ω_2^{F} denote the subdomains sharing F as their common face, and let $\mathscr{A}_{\mathrm{F}}$ and $\mathscr{A}_{ll}$ be the stiffness matrices generated by the basis functions on F and in

$\Omega_l^{\rm F}$ $(l=1,2)$, respectively. Then the equation (4.4) can be transformed into the algebraic system

$$\begin{pmatrix} \mathscr{A}_{11} & \mathbf{0} & \mathscr{A}_{1\rm F} \\ \mathbf{0} & \mathscr{A}_{22} & \mathscr{A}_{1\rm F} \\ \mathscr{A}_{1\rm F}^t & \mathscr{A}_{2\rm F}^t & \mathscr{A}_{\rm F} \end{pmatrix} \begin{pmatrix} \mathcal{X}_1^{\rm F} \\ \mathcal{X}_2^{\rm F} \\ \mathcal{X}_{\rm F} \end{pmatrix} = \begin{pmatrix} \mathbf{0} \\ \mathbf{0} \\ b_{\rm F} \end{pmatrix}, \tag{4.5}$$

where $\mathcal{X}_{\rm F}$ denote the dofs (i.e., coordinate vector) of $\mathbf{u}_{\rm F}$ on F, and $b_{\rm F}$ is defined by

$$b_{\rm F} = \xi_{\rm F} - \mathscr{A}_{1\rm F}^t \xi_1^{\rm F} - \mathscr{A}_{2\rm F}^t \xi_2^{\rm F},$$

with $\xi_{\rm F}$ being the dofs of $\mathbf{g}$ on F, and $\xi_l^{\rm F}$ being the dofs of $\mathbf{u}_l$ in $\Omega_l^{\rm F}$ $(l=1,2)$.

It is easy to see that the system (4.5) is the same as the algebraic system of the original equation (2.2) restricted in $V_h^0(\Omega_{\rm F})$, with different right hand only. Notice that, as in Step 4 of **Algorithm 3.1**, the dofs. in the interior of the subdomain $\Omega_l^{\rm F}$ can be gotten by computing the local harmonic extension in $\Omega_l^{\rm F}$ $(l=1,2)$. Thus we only hope to get a rough approximation of $\mathcal{X}_{\rm F}$ but do not care for the accuracy of $\mathcal{X}_l^{\rm F}$ $(l=1,2)$. Intuitively, the accuracy of an approximation for $\mathcal{X}_{\rm F}$ mainly depends on the grids nearing F and is not sensitive to the grids far from F. Based on this observation, we can construct an auxiliary non-uniform partition $\tilde{\mathcal{T}}_{\tilde{h}}^{\rm F}$ on $\Omega_{\rm F}$, for which the original fine grids on F are kept and the grids in $\Omega_l^{\rm F}$ $(l=1,2)$ gradually becomes coarser when nodes are far from F. Then we solve the following auxiliary algebraic system

$$\begin{pmatrix} \tilde{\mathscr{A}}_{11}^{\rm F} & \mathbf{0} & \tilde{\mathscr{A}}_{1\rm F} \\ \mathbf{0} & \tilde{\mathscr{A}}_{22}^{\rm F} & \tilde{\mathscr{A}}_{1\rm F} \\ \tilde{\mathscr{A}}_{1\rm F}^t & \tilde{\mathscr{A}}_{2\rm F}^t & \mathscr{A}_{\rm F} \end{pmatrix} \begin{pmatrix} \tilde{\mathcal{X}}_1^{\rm F} \\ \tilde{\mathcal{X}}_2^{\rm F} \\ \tilde{\mathcal{X}}_{\rm F} \end{pmatrix} = \begin{pmatrix} \mathbf{0} \\ \mathbf{0} \\ b_{\rm F} \end{pmatrix}, \tag{4.6}$$

where $\tilde{\mathscr{A}}_{ll}^{\rm F}$ denotes the stiffness matrix generated by the basis functions associated with the auxiliary grids in $\Omega_l^{\rm F}$ $(l=1,2)$. The solution $\tilde{\mathcal{X}}_{\rm F}$ of the above system can be regarded as a rough approximation of $\mathcal{X}_{\rm F}$. The auxiliary partition $\tilde{\mathcal{T}}_{\tilde{h}}^{\rm F}$ (see Fig. 3) can be easily generated by the existing software [25], such that the number of the unknowns in (4.6) is much smaller than that in (4.5), so the system (4.6) is very cheap to solve.

Associated with each $\hat{V}_h^{\perp}(\Omega_{\rm V})$, we can similarly define an auxiliary partition $\tilde{\mathcal{T}}_{\tilde{h}}^{\rm V}$ (see Fig. 3), and build the corresponding algebraic system

$$\begin{pmatrix} \tilde{\mathscr{A}}_{11}^{\rm V} & \mathbf{0} & \cdots & \mathbf{0} & \tilde{\mathscr{A}}_{1\rm V} \\ \mathbf{0} & \tilde{\mathscr{A}}_{22}^{\rm V} & \cdots & \mathbf{0} & \tilde{\mathscr{A}}_{2\rm V} \\ \vdots & \vdots & \vdots & \vdots & \vdots \\ \mathbf{0} & \cdots & \mathbf{0} & \tilde{\mathscr{A}}_{mm}^{\rm V} & \tilde{\mathscr{A}}_{m\rm V}^t \\ \tilde{\mathscr{A}}_{1\rm V}^t & \tilde{\mathscr{A}}_{2\rm V}^t & \cdots & \tilde{\mathscr{A}}_{m\rm V}^t & \mathscr{A}_{\rm V} \end{pmatrix} \begin{pmatrix} \tilde{\mathcal{X}}_1^{\rm V} \\ \tilde{\mathcal{X}}_2^{\rm V} \\ \vdots \\ \tilde{\mathcal{X}}_m^{\rm V} \\ \tilde{\mathcal{X}}_{\rm V} \end{pmatrix} = \begin{pmatrix} \mathbf{0} \\ \mathbf{0} \\ \vdots \\ \mathbf{0} \\ b_{\rm V} \end{pmatrix}, \tag{4.7}$$

where $\mathscr{A}_{\rm V}$ is the stiffness matrix generated by the basis functions associated with the grids on $W_{\rm V}^{half}$, and $\tilde{\mathcal{X}}_{\rm V}$ denotes an approximation of the dofs. of $\mathbf{u}_{\rm V}$ on $W_{\rm V}^{half}$.

Here $\mathbf{u}_{\mathrm{V}} \in \hat{V}_h^0(\Omega_{\mathrm{V}})$ is defined by

$$\mathcal{A}(\mathbf{u}_{\mathrm{V}}, \mathbf{w}) = (\mathbf{g}, \mathbf{w}) - \sum_{k \in \Lambda_{\mathrm{V}}} \mathcal{A}(\mathbf{u}_k, \mathbf{w}), \ \forall \mathbf{w} \in \hat{V}_h^0(\Omega_{\mathrm{V}})$$

with

$$\hat{V}_h^0(\Omega_{\mathrm{V}}) = \{\mathbf{v} \in V_h^0(\Omega_{\mathrm{V}}) : \text{ the trace of } \mathbf{v} \text{ belongs to } \hat{V}_h^0(\Gamma_{\mathrm{V}}^{half})\}.$$

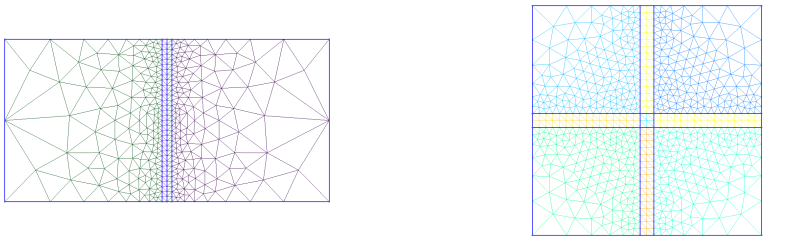

(a) $\tilde{\mathcal{T}}_{\tilde{h}}^{\mathrm{F}}$ (b) $\tilde{\mathcal{T}}_{\tilde{h}}^{\mathrm{V}}$

FIGURE 3. 2D cross-sections of coarsening grids for Ω_{F} and $\Omega_{\mathrm{V}}^{half}$

According to the above discussions, the approximate solvers $\tilde{A}_{\mathrm{F}} : V_h^{\perp}(\Omega_{\mathrm{F}}) \to V_h^{\perp}(\Omega_{\mathrm{F}})$ and $\tilde{A}_{\mathrm{V}} : \hat{V}_h^{\perp}(\Omega_{\mathrm{V}}) \to \hat{V}_h^{\perp}(\Omega_{\mathrm{V}})$ can be defined as follows: for $\mathbf{g} \in V_h^{\perp}(\Omega_{\mathrm{F}})$, we define $\tilde{\mathbf{u}}_{\mathrm{F}} = \tilde{A}_{\mathrm{F}}^{-1}\mathbf{g} \in V_h^{\perp}(\Omega_{\mathrm{F}})$ and $\tilde{\mathbf{u}}_{\mathrm{V}} = \tilde{A}_{\mathrm{V}}^{-1}\mathbf{g} \in \hat{V}_h^{\perp}(\Omega_{\mathrm{V}})$, such that the dofs of $\tilde{\mathbf{u}}_{\mathrm{F}}$ on F and W_{V}^{half} equal to $\tilde{\mathcal{X}}_{\mathrm{F}}$ and $\tilde{\mathcal{X}}_{\mathrm{V}}$ computed by solving (4.6) and (4.7), respectively.

Remark 4.1. *The construction of the above approximate solvers do not depend on the original bilinear form $\mathcal{A}(\cdot,\cdot)$ and the interior grids of the subdomains for coarsening. Thus we need not to estimate the norm induced from $\mathcal{A}(\cdot,\cdot)$ on F and W_{V}^{half}, and need not to give special assumptions on the original grids.*

Remark 4.2. *For the coarsening technique introduced in this subsection, the grids on the considered local interface with non-zero dofs need to be kept, so the number of nodes on such an interface should be much smaller than that on the boundary of every subdomain for coarsening, otherwise, the number of nodes of the coarsening partition is still great (see the data in Subsection 6.4). Because of this, we did not make the coarsening directly for the original space $V_h^{\perp}(\Omega_{\mathrm{V}})$ defined in Subsection 3.1, and we have to build the decomposition (4.1) and define the spaces $\hat{V}_h^{\perp}(\Omega_{\mathrm{V}})$ and $V_h^{\perp}(\Omega_{\mathrm{F}})$. Of course, if there is no degree of freedom on the edges in $\mathcal{E}_{\mathrm{V}}$ (Raviart-Thomas elements), then we need not to define the space $\hat{V}_h^{\perp}(\Omega_{\mathrm{V}})$ (which only grasps the degrees of freedom on coarse edges). For this case, the second sum in (4.3) will not appear.*

4.2. **Preconditioner.** By using the space decomposition in Subsection 4.1 and the approximate interface solvers in Subsection 4.2, we can define the second preconditioner for A as

$$B_{II}^{-1} = B_d^{-1}Q_d + \sum_{k=1}^{N} A_k^{-1}Q_k + \sum_{\mathrm{V}\in\mathcal{N}_d} \tilde{A}_{\mathrm{V}}^{-1}Q_{\mathrm{V}} + \sum_{\mathrm{F}\in\mathcal{F}_d} \tilde{A}_{\mathrm{F}}^{-1}Q_{\mathrm{F}}. \tag{4.8}$$

When there is no degree of freedom on the edges in $\mathcal{E}_{\mathrm{V}}$ (Raviart-Thomas elemens), the second sum in the preconditioner would be dropped.

The action of B_{II}^{-1} can be described by the following algorithm.

Algorithm 4.1. For $\mathbf{g} \in V_h(\Omega)$, we can compute $\mathbf{u} = B_{II}^{-1}\mathbf{g}$ in five steps.

Step 1. Solve the system of $\mathbf{u}_d \in V_d(\Omega)$:

$$\mathcal{A}(\mathbf{u}_d, \mathbf{v}_d) = (\mathbf{g}, \mathbf{v}_d),\ \forall \mathbf{v}_d \in V_d(\Omega);$$

Step 2. Solve the following systems of $\mathbf{u}_k \in V_h^0(\Omega_k)$ in parallel:

$$\mathcal{A}(\mathbf{u}_k, \mathbf{v}) = (\mathbf{g}, \mathbf{v}),\ \forall \mathbf{v} \in V_h^0(\Omega_k)\ (k = 1, \cdots, N);$$

Step 3. Solve the system (4.6) to get the dofs $\tilde{\mathcal{X}}_{\mathrm{F}}$ of $\tilde{\mathbf{u}}_{\mathrm{F}}$ on F in parallel for every $\mathrm{F} \in \mathcal{F}_{\mathrm{V}}$;

Step 4. Solve the system (4.7) to get the dofs $\tilde{\mathcal{X}}_{\mathrm{V}}$ of $\tilde{\mathbf{u}}_{\mathrm{V}}$ on W_{V}^{half} in parallel for every $\mathrm{V} \in \mathcal{N}_d$;

Step 5. Use all $\tilde{\mathcal{X}}_{\mathrm{F}}$ and $\tilde{\mathcal{X}}_{\mathrm{V}}$ to get the dofs. $\tilde{\mathcal{X}}_{\partial\Omega_k}$ of $\sum_{\mathrm{F}\subset\partial\Omega_k} \tilde{\mathbf{u}}_{\mathrm{F}} + \sum_{\mathrm{V}\in\partial\Omega_k} \tilde{\mathbf{u}}_{\mathrm{V}}$ on $\partial\Omega_k$. Compute the discrete A-extension $\mathbf{u}_k^{\perp}$ in parallel, such that $\mathbf{u}_k^{\perp}$ has the dofs $\tilde{\mathcal{X}}_{\partial\Omega_k}$ on $\partial\Omega_k$ and satisfies

$$\mathcal{A}(\mathbf{u}_k^{\perp}, \mathbf{v}) = 0,\ \forall \mathbf{v} \in V_h^0(\Omega_k)\ (k = 1, \cdots, N).$$

Finally, we define

$$\mathbf{u} = \mathbf{u}_d + \sum_{k=1}^{N} (\mathbf{u}_k + \mathbf{u}_k^{\perp}).$$

Remark 4.3. *The essential difference between the proposed substructuring method and the existing substructuring methods is that novel local interface solvers are used in Step 3 and Step 4 of the above algorithm. As explained in Subsection 4.2, the interface solvers are cheap and easy to implement. In fact, the auxiliary subproblems needed to be solved in Step 3 and Step 4 have very small dofs. (see the data in Section 6). When there is no degree of freedom on the edges in $\mathcal{E}_{\mathrm{V}}$ (Raviart-Thomas elemens), we need not to implement Step 4. Notice that the local problems in Step 5 have the same stiffness matrices with that in Step 2 (with different right hands only). Thus the implementation of Step 5 is very cheap by using LU decomposition made in Step 2 for each local stiffness matrix.*

5. Applications

In this section, we introduce two typical elliptic-type equations.

5.1. **Linear elasticity problems.** Let's consider the linear elasticity problem:

$$\begin{cases} -\sum\limits_{j=1}^{3} \frac{\partial \sigma_{ij}}{\partial x_j}(\boldsymbol{u}) = f_i, \quad in\ \Omega \\ \qquad\qquad \boldsymbol{u} = 0, \quad on\ \partial\Omega \end{cases} \tag{5.1}$$

where $\boldsymbol{f} = (f_1\ f_2\ f_3)^T$ is an internal volume force, e.g. gravity (cf. [9]). The linearized strain tensor is defined by

$$\varepsilon = \varepsilon(\boldsymbol{u}) = [\varepsilon_{ij} = \frac{1}{2}(\frac{\partial u_i}{\partial x_i} + \frac{\partial u_j}{\partial x_i})]$$

and

$$\sigma_{ij}(\boldsymbol{u}) := \lambda \delta_{ij} div\boldsymbol{u} + 2\mu\varepsilon_{ij},$$

where λ and μ are the *Lamé* parameters (cf. [44]), which are positive functions.

As usual, let $H_0^1(\Omega) \subset H^1(\Omega)$ denote the space consisting of the functions having the zero trace on $\partial\Omega$. We introduce the vector value Sobolev space $(H_0^1(\Omega))^3$, equipped with the usual product norm as follows:

$$||\boldsymbol{u}||_{1,\Omega} := (|\boldsymbol{u}|^2_{H^1(\Omega)} + ||\boldsymbol{u}||^2_{L_2(\Omega)})^{\frac{1}{2}}$$

with $||\boldsymbol{u}||^2_{L_2(\Omega)} := \int_\Omega |\boldsymbol{u}|^2 dx$ and $|\boldsymbol{u}|^2_{H^1(\Omega)} := ||\nabla \boldsymbol{u}||^2_{L_2(\Omega)}$. Concerning the variational problem (2.1), we have $V(\Omega) := [H_0^1(\Omega)]^3$,

$$\boldsymbol{\mathcal{A}}(\boldsymbol{u}, \boldsymbol{v}) = \int_\Omega (2\mu\varepsilon(\boldsymbol{u}) : \varepsilon(\boldsymbol{v}) + \lambda div\boldsymbol{u} \cdot div\boldsymbol{v}) dx$$

and

$$\langle \boldsymbol{F}, \boldsymbol{v} \rangle = \int_\Omega \boldsymbol{f} \cdot \boldsymbol{v} dx$$

with

$$\varepsilon(\boldsymbol{u}) : \varepsilon(\boldsymbol{v}) := \sum_{i,j=1}^{n} \varepsilon_{ij}(\boldsymbol{u})\varepsilon_{ij}(\boldsymbol{v}).$$

Let $R(K)$ be a subset of all linear polynomials on the element K of the form:

$$R(K) = \Big\{ \boldsymbol{A} \cdot \mathbf{x} + \boldsymbol{C};\ \boldsymbol{A} \in \mathbb{R}^{3\times 3}, \boldsymbol{C} \in \mathbb{R}^3,\ \mathbf{x} \in K \Big\}.$$

Assume that Ω can be written as the union of polyhedral subdomains $D_1, \cdots, D_{N_0}$, such that $\lambda(x) = \lambda_r$ and $\mu(x) = \mu_r$ for $x \in D_r$, with λ_r and μ_r being positive constants. In applications, N_0 is a *fixed* positive integer, so the diameter of each D_r is $O(1)$. It is certain that the subdomains Ω_k should satisfy the condition: each D_r is the union of some subdomains in $\{\Omega_k\}$.

5.2. **Maxwell's equations.** For the time-dependent Maxwell's equations, we need to solve the following **curlcurl**-system at each time step (see [6, 27, 40]):

$$\begin{cases} \mathbf{curl}(\alpha\,\mathbf{curl}\,\mathbf{u}) + \beta\mathbf{u} = \mathbf{f}, & in \quad \Omega, \\ \mathbf{u}\times\boldsymbol{n} = 0, & on \quad \partial\Omega \end{cases} \tag{5.2}$$

where the coefficients $\alpha(\mathbf{x})$ and $\beta(\mathbf{x})$ are two positive bounded functions in Ω, and $\mathbf{n}$ is the unit outward normal vector on $\partial\Omega$.

Let $H(\mathbf{curl};\Omega)$ be the Sobolev space consisting of all square integrable functions whose **curl**'s are also square integrable in Ω, and $H_0(\mathbf{curl};\Omega)$ be the subspace of $H(\mathbf{curl};\Omega)$ of all functions whose tangential components vanishing on $\partial\Omega$. In order to get the weak form of (5.2), just like linear elasticity problems, we define $V(\Omega) = H_0(\mathbf{curl})$,

$$\boldsymbol{\mathcal{A}}(\boldsymbol{u},\boldsymbol{v}) = \int_\Omega (\alpha\ \mathbf{curl}\ \mathbf{u}\cdot\mathbf{curl}\ \mathbf{v} + \beta\ \mathbf{u}\cdot\mathbf{v})dx$$

and

$$\langle \boldsymbol{F},\boldsymbol{v}\rangle = \int_\Omega \mathbf{f}\cdot\boldsymbol{v}dx.$$

Let $R(K)$ be a subset of all linear polynomials on the element K of the form:

$$R(K) = \left\{\mathbf{a}+\mathbf{b}\times\mathbf{x};\ \mathbf{a},\mathbf{b}\in\mathbb{R}^3,\ \mathbf{x}\in K\right\}.$$

It is well-known that for any $\mathbf{v}\in V_h(\Omega)$, its tangential components are continuous on all edges of each element in the triangulation $\mathcal{T}_h$. Moreover, each edge element function $\mathbf{v}$ in $V_h(\Omega)$ is uniquely determined by its moments on each edge e of $\mathcal{T}_h$:

$$\left\{\lambda_e(\mathbf{v}) = \int_e \mathbf{v}\cdot\mathbf{t}_e ds;\ e\in\mathcal{E}_h\right\}, \tag{5.3}$$

where $\mathbf{t}_e$ denotes the unit vector on the edge e.

As in the last subsection, we assume that Ω can be written as the union of polyhedral subdomains $D_1,\cdots,D_{N_0}$ with N_0 being a fixed positive integer, such that $\alpha(x)=\alpha_r$ and $\beta(x)=\beta_r$ for $x\in D_r$, where every α_r and β_r is a positive constant. Let the subdomains Ω_k satisfy the condition: each D_r is the union of some subdomains in $\{\Omega_k\}$.

6. Numerical Experiments

In this section, we report some numerical results to illustrate the effectiveness of the proposed substructuring preconditioners.

We consider the models introduced in Section 5, with $\Omega=(0,1)^3$, and we make tests for different distributions of the coefficients $\lambda(x)$, $\mu(x)$, $\alpha(\mathbf{x})$ and $\beta(\mathbf{x})$:

Case (i): the coefficients have no jump, i.e., $\lambda(x)=\mu(x)=1$ (linear elasticity problems) or $\alpha(\mathbf{x})=\beta(\mathbf{x})=1$ (Maxwell's equations).

Case (ii): the coefficients have large jumps, i.e.,

$$\lambda(\mathbf{x}) = \begin{cases} \lambda_0, & in\ D \\ \\ 1, & in\ \Omega\backslash D, \end{cases} \qquad \mu(\mathbf{x}) = \begin{cases} \mu_0, & in\ D, \\ \\ 1, & in\ \Omega\backslash D \end{cases}$$

for linear elasticity problems and

$$\alpha(\mathbf{x}) = \begin{cases} \alpha_0, & in\ D \\ \\ 1, & in\ \Omega\backslash D, \end{cases} \qquad \beta(\mathbf{x}) = \begin{cases} \beta_0, & in\ D, \\ \\ 1, & in\ \Omega\backslash D \end{cases}$$

for Maxwell's equations. Here $D \subset \Omega$ is a union of several subdomains Ω_k. We consider two choices of D:

$$\text{Choice (1). } D = [\frac{1}{4},\ \frac{1}{2}]^3;\ \text{Choice (2). } D = [\frac{1}{4},\ \frac{1}{2}]^3 \bigcup [\frac{1}{2},\ \frac{3}{4}]^3.$$

In our experiments, we define domain decomposition and finite element partition as follows. At first, we divide the domain into n^3 smaller cubes Ω_1, $\Omega_2 \cdots \Omega_N$, which have the same length d of edges, i.e., $d = 1/n$. We require that $D \subset \Omega$ is just the union of some subdomains in $\{\Omega_k\}$, which yields the desired domain decomposition. Next, we divide each subdomain Ω_k into m^3 fine cubes, with the same size $h = 1/(mn)$. All the fine cubes constitute a partition $\mathcal{T}_h$ consisting of hexahedral elements. If we further divide each fine cube into 5 or 6 tetrahedrons in the standard way, then all the generated tetrahedrons constitute a partition $\mathcal{T}_h$ consisting of tetrahedral elements.

We discretize the models by the linear finite element methods, and we apply the PCG method with the proposed preconditioners to solve the resulting algebraic systems. The PCG iteration is terminated in our experiments when the relative residual is less than 10^{-6}. We will report the iteration counts in the rest of this section.

6.1. **Tests for linear elasticity problems.** In this subsection, we consider an example of the linear elasticity problem. We choose the right-hand side $\boldsymbol{f}$ of system (5.1) such that the analytic solution $\mathbf{u} = (u_1, u_2, u_3)^T$ is given by:

$$\begin{aligned} u_1 &= x(x-1)y(y-1)z(z-1) \\ u_2 &= x(x-1)y(y-1)z(z-1) \\ u_3 &= x(x-1)y(y-1)z(z-1) \end{aligned}$$

where the coefficients $\lambda(x) = \mu(x) = 1$. In our experiments, the right-hand side $\boldsymbol{f}$ is fixed.

6.1.1. *Efficiency of the first preconditioner.* In this part, we test the action of the preconditioner B_I described by **Algorithm 3.1**. We use both hexahedral partition and tetrahedral partition in our experiments. We first consider the case of hexahedral partition. The iteration counts of the PCG method with B_I are listed in Table 1 (for **Case** (i)) and Table 2 (for **Case** (ii)).

TABLE 1
Iteration counts of PCG with the preconditioner B_I (hexahedral elements): the coefficients have no jumps

$m\backslash n$	4	6	8	10
4	15	15	15	14
8	16	16	16	16
16	18	18	19	19
32	21	21	21	21

TABLE 2
Iteration counts of PCG with the preconditioner B_I (hexahedral elements): the coefficients have large jumps

	Choice (1) of D				Choice (2) of D			
	$\lambda_0=\mu_0=10^{-5}$		$\lambda_0=\mu_0=10^{5}$		$\lambda_0=\mu_0=10^{-5}$		$\lambda_0=\mu_0=10^{5}$	
$m \setminus n$	4	8	4	8	4	8	4	8
8	14	16	19	19	14	16	18	19
16	16	19	22	21	16	19	21	21
24	18	21	23	23	18	21	23	23
32	19	22	26	24	18	22	24	24

We observe from Table 1 that, when the coefficients is smooth, the iteration counts of PCG method grows slowly when $m = d/h$ increases but $n = 1/d$ is fixed, and almost unchange when m is fixed but n increases. The data in Table 2 indicate that, even if the coefficients have large jumps, the iteration counts of PCG still grows slowly. It confirms that the preconditioner B_I is effective for the system arising from nodal element discretization for linear elasticity problems.

Next we consider the case with tetrahedral partition. Since the subdomains are hexahedrons, the coarse space associated with the subdomains is not a subspace of the fine tetrahedral element space. Because of this, we further divide each cubic subdomain into 5 or 6 tetrahedrons, and use all the tetrahedral subdomains to define a nested coarse space. Notice that the resulting tetrahedral coarse space has

the same number of the degrees of freedom as the original hexahedral coarse space, i.e., this change will not increase the cost for implementing the coarse solver.

We list the iteration counts of the PCG method with B_I in Table 3 (for **Case** (i)) and Table 4 (for **Case** (ii)).

TABLE 3
Iteration counts of PCG with the preconditioner B_I (tetrahedral elements): the coefficients have no jump

$m\backslash n$	4	6	8	10
8	20	20	20	19
16	23	23	22	21
24	24	24	23	23
32	25	25	24	24

TABLE 4
Iteration counts of PCG with the preconditioner B_I (tetrahedral elements): the coefficients have large jumps

	Choice (1) of D				Choice (2) of D			
	$\lambda_0=\mu_0=10^{-5}$		$\lambda_0=\mu_0=10^{5}$		$\lambda_0=\mu_0=10^{-5}$		$\lambda_0=\mu_0=10^{5}$	
$m \setminus n$	4	8	4	8	4	8	4	8
8	17	20	27	23	17	21	27	23
16	20	22	29	25	20	24	29	25
24	21	24	31	27	21	25	31	27
32	22	25	32	28	22	26	32	28

We observe that the iteration counts of PCG in these two tables vary stably for the considered two cases (even if the coefficents have large jumps). In addition, we can see that the convergence rate of PCG is same as in the case with the hexahedron elements.

6.1.2. *Efficiency of the second preconditioner.* In this subsection we investigate the efficiency of the preconditioner B_{II} described by **Algorithm 4.1**.

Firstly, we consider the case of hexahedral elements. The iteration counts of the PCG method with B_{II} are listed in Table 5 (for **Case** (i)) and Table 6 (for **Case** (ii)).

TABLE 5

Iteration counts of PCG with the preconditioner B_{II} (hexahedral elements): the coefficients have no jump

$m\backslash n$	4	6	8	10
8	19	19	19	19
16	22	22	22	22
24	24	24	24	23
32	25	25	24	24

TABLE 6
Iteration counts of PCG with the preconditioner B_{II} (hexahedral elements): the coefficients have large jumps

	Choice (1) of D				Choice (2) of D			
	$\lambda_0 = \mu_0 = 10^{-5}$		$\lambda_0 = \mu_0 = 10^5$		$\lambda_0 = \mu_0 = 10^{-5}$		$\lambda_0 = \mu_0 = 10^5$	
$m \backslash n$	4	8	4	8	4	8	4	8
8	17	20	24	23	17	20	25	23
16	20	24	28	27	20	24	28	27
24	22	26	30	29	22	26	31	29
32	23	27	31	30	23	27	32	30

From Table 5, we observe that the rate of convergence of PCG with B_{II} is same as that with B_I. In addition, we found that the iteration counts in Table 5 are slightly more than that in Table 1 when the values of m, n are same in these two tables. But in each PCG iteration step, the calculation of $B_{II}^{-1}g$ is much cheaper than $B_I^{-1}g$ when d/h is large enough (we will investigate this question in the final subsection of this section). We can see from Table 6 that, even if coefficients have large jumps, the iteration counts vary stably. This means that the preconditioner B_{II} is not only cheaper, but also effective for elasticity problems.

Next we consider the case of tetrahedral partition. Here we construct a coarse space as in the last subsection for B_I. The iteration counts of the PCG are listed in Table 7 (for **Case** (i)) and Table 8 (for **Case** (ii)).

TABLE 7
Iteration counts of PCG with the preconditioner B_{II} (tetrahedral elements): the coefficients have no jump

$m\backslash n$	4	6	8	10
8	22	22	21	21
16	25	25	24	24
24	27	27	26	25
32	29	28	27	27

TABLE 8
Iteration counts of PCG with the preconditioner B_{II} (tetrahedral elements): the coefficients have large jumps

	Choice (1) of D				Choice (2) of D			
	$\lambda_0 = \mu_0 = 10^{-5}$		$\lambda_0 = \mu_0 = 10^{5}$		$\lambda_0 = \mu_0 = 10^{-5}$		$\lambda_0 = \mu_0 = 10^{5}$	
$m \backslash n$	4	8	4	8	4	8	4	8
8	19	22	31	26	19	23	30	27
16	23	27	35	30	22	27	34	31
24	24	29	37	32	24	29	37	33
32	26	31	39	34	26	31	39	35

Like the case of hexahedral elements, the preconditioner B_{II} is still effective for the case of tetrahedral elements.

6.2. **Tests for Maxwell's equations.** In this subsection, we consider Maxwell's equations. Let the right-hand side $\boldsymbol{f}$ in the equations (5.2) to be selected such that the exact solution $\mathbf{u} = (u_1, u_2, u_3)^T$ is given by

$$\begin{aligned} u_1 &= xyz(x-1)(y-1)(z-1)\,, \\ u_2 &= \sin(\pi x)\sin(\pi y)\sin(\pi z)\,, \\ u_3 &= (1-e^{x})(1-e^{x-1})(1-e^{y})(1-e^{y-1})(1-e^{z})(1-e^{z-1})\,, \end{aligned}$$

where the coefficients $\alpha(\mathbf{x})$ and $\beta(\mathbf{x})$ are both constant 1. This right-hand side $\boldsymbol{f}$ is also fixed in our experiments.

6.2.1. *Efficiency of the first preconditioner.* In this part, we investigate the effectiveness of the preconditioner B_I described by **Algorithm 3.1**. We first consider the case of hexahedral elements. The iteration counts of the PCG method with B_I are listed in Table 9 (for **Case** (i)) and Table 10 (for **Case** (ii)).

TABLE 9
Iteration counts of PCG with the preconditioner B_I (hexahedral elements): the coefficients have no jump

$m\backslash n$	4	6	8	10
8	16	15	15	15
16	17	18	18	17
24	19	19	19	18
32	20	20	20	20

TABLE 10
Iteration counts of PCG with the preconditioner B_I (hexahedral elements): the coefficients have large jumps

	Choice (1) of D				Choice (2) of D			
	$\beta_0 = \alpha_0 = 10^{-5}$		$\beta_0 = \alpha_0 = 10^{5}$		$\beta_0 = \alpha_0 = 10^{-5}$		$\beta_0 = \alpha_0 = 10^{5}$	
$m \backslash n$	4	8	4	8	4	8	4	8
8	13	15	19	17	13	15	19	19
16	15	17	21	20	15	17	22	22
24	16	18	23	21	16	19	24	24
32	16	19	24	22	16	19	25	25

We observe from the above two tables that, although the coarse space is chosen as the simplest one for Maxwell's equations, the iteration counts of the PCG method with the preconditioner B_I grow logarihmically with $m = d/h$ only, not depend on $n = 1/d$, even if the coefficients have large jumps.

Now we consider the case of tetrahedral elements. For this case, we can not simply consider the coarse space corresponding to the hexahedral subdomain partition. If we divide each hexahedral subdomain into 5 or 6 tetrahedral subdomains and use the tetrahedral coarse space as in the last section, then the tetrahedral coarse space have much more degrees of freedom than the natural hexahedral coarse space, since the degrees of freedom are defined on the coarse edges for Maxwell's equations. A natural idea is to define a tetrahedral coarse space as the image space of the interpolation operator acting on the natural hexahedral coarse space. Then the degrees of freedom are not increased in the resulting tetrahedral coarse space. The iteration counts of the PCG method are listed in Table 11 (for **Case** (i)) and Table 12 (**Case** (ii)).

TABLE 11
Iteration counts of PCG with the preconditioner B_I (tetrahedral elements): the coefficients have no jump

$m\backslash n$	4	6	8	10
8	18	17	17	16
16	20	20	19	19
24	22	21	21	21
32	22	22	22	21

TABLE 12
Iteration counts of PCG with the preconditioner B_I (tetrahedral elements): the coefficients have large jumps

	Choice (1) of D				Choice (2) of D			
	$\beta_0 = \alpha_0 = 10^{-5}$		$\beta_0 = \alpha_0 = 10^{5}$		$\beta_0 = \alpha_0 = 10^{-5}$		$\beta_0 = \alpha_0 = 10^{5}$	
$m \backslash n$	4	8	4	8	4	8	4	8
8	15	17	21	20	15	17	21	21
16	17	20	24	22	17	20	24	24
24	18	21	25	23	18	21	26	26
32	19	22	26	24	19	22	27	28

From the above two tables, we can see that the iteration counts vary stably and the PCG iteration has the same convergence rate as in the case of the linear elasticity problem.

6.2.2. *Efficiency of the second preconditioner.* In this part, we investigate the effectiveness B_{II} for the case of Maxwell's equations.

Firstly, we consider the hexahedral partition. We list the iteration counts of PCG method in Table 13 (for **Case** (i)) and Table 14 (for **Case** (ii)).

TABLE 13
Iteration counts of PCG with the preconditioner B_{II} (hexahedral elements): the coefficients have no jump

$m\backslash n$	4	6	8	10
8	23	22	21	21
16	23	23	22	21
24	25	25	24	23
32	26	26	25	24

TABLE 14

Iteration counts of PCG with the preconditioner B_{II} (hexahedral elements): the coefficients have large jumps

	Choice (1) of D				Choice (2) of D			
	$\beta_0 = \alpha_0 = 10^{-5}$		$\beta_0 = \alpha_0 = 10^{5}$		$\beta_0 = \alpha_0 = 10^{-5}$		$\beta_0 = \alpha_0 = 10^{5}$	
$m \backslash n$	4	8	4	8	4	8	4	8
8	18	21	27	25	18	21	27	29
16	19	21	29	26	19	21	29	28
24	21	23	31	28	21	24	31	31
32	21	25	33	30	21	25	33	34

From above table, we observe that the convergence rate of PCG method with the preconditioner B_{II} is quasi-optimal, even if the coefficients have large jumps.

Next we consider the case of the tetrahedral elements. We use the same way to define a coarse space as in Subsection 6.2.1 for this case. We list the iteration counts of PCG method with the preconditioner B_{II} in Table 15 (for **Case (i)**) and Table 16 (for **Case (ii)**).

TABLE 15
Iteration counts of PCG with the preconditioner B_{II} (tetrahedral elements): the coefficients have no jump

$m\backslash n$	4	6	8	10
8	21	21	20	20
16	26	25	24	24
24	26	25	24	24
32	28	28	27	26

TABLE 16
Iteration counts of PCG with the preconditioner B_{II} (tetrahedral elements): the coefficients have large jumps

	Choice (1) of D				Choice (2) of D			
	$\beta_0 = \alpha_0 = 10^{-5}$		$\beta_0 = \alpha_0 = 10^{5}$		$\beta_0 = \alpha_0 = 10^{-5}$		$\beta_0 = \alpha_0 = 10^{5}$	
$m\backslash n$	4	8	4	8	4	8	4	8
8	18	20	27	24	18	20	26	26
16	21	24	32	29	21	24	32	31
24	21	23	32	28	21	23	31	31
32	23	27	35	32	23	27	35	35

It can be seen from the above two tables that the iteration counts of the PCG method with the new preconditioner only slowly grow when $m = d/h$ increases, but not depend on $n = 1/d$.

6.3. **On the proposed coarsening technique.** It can be seen, from the results in Subsection 6.1 and Subsection 6.2, that the preconditioner B_{II} has almost the same convergence rate as the preconditioner B_I. A key ingredient in the preconditioner B_{II} is the proposed coarsening technique. In this subsection, we give some numerical result to illustrate the efficiency of the coarsening technique and further explain that the preconditioner B_{II} is indeed very cheap.

We first consider a typical cuboid domain $G = [0, 2] \times [0, 1] \times [0, 1]$ to investigate the approximate effect of the coarsening technique. Let G be divided into the union of two cube G_1 and G_2, with $G_1 = [0, 1]^3$ and $G_2 = [1, 2] \times [0, 1] \times [0, 1]$, and set $\mathrm{F} = \partial G_1 \cap \partial G_2$. We will compare the accuracy of the solutions of the two systems (4.5) (with the original partition $\mathcal{T}_h$) and (4.6) (with the coarsening partition $\tilde{\mathcal{T}}_h^{\mathrm{F}}$), where $\Omega_l^{\mathrm{F}} = G_l$ $(l = 1, 2)$. To this end, we need to calculate the discrete l^2 relative error on F, which is defined by

$$err. = \frac{||\tilde{\mathcal{X}}_{\mathrm{F}} - \mathcal{X}_{\mathrm{F}}||_{l^2}}{||\mathcal{X}_{\mathrm{F}}||_{l^2}}.$$

In Table 17, we list the results for the linear elasticity problem and Maxwell's equations, with constant coefficients.

TABLE 17
The l^2 relative error restricted on the interface F for coarsening

	$err.$	
h	Linear elasticity problem	Maxwell's equations
1/8	0.0407	0.0582
1/16	0.0240	0.0317
1/24	0.0225	0.0284
1/32	0.0233	0.0254

From this table, we can see that the solution of the auxiliary system (4.6) indeed is a rough approximation of the solution of the interface system (4.5), which can explain why the preconditioner B_{II} is effective, as confirmed in Subsection 6.1.2 and Subsection 6.2.2.

Next, we illustrate the local solvers in B_{II} indeed is very cheap. For simplicity, we just select one face F and one interior vertex $\mathrm{V} \in \mathcal{N}_d$ to test our coarsening technique, where the face F is shared by Ω_i and Ω_j. Let n_c and n_f denote the dofs corresponding to the coarsening partition and the original fine partition on Ω_{F} (or Ω_{V}), respectively.

In Table 18 and Table 19, we list the local dofs n_c and n_f for linear elasticity problem and Maxwell's equations, respectively.

TABLE 18
The dofs of local problems solved in Step 3 and Step 4 of **Algorithm 4.1**: linear elasticity problem (with vector-valued nodal basis functions)

	Ω_{F}			$\Omega_{\mathrm{V}}^{half}$		
d/h	n_c (coarse)	n_f (fine)	n_c/n_f	n_c (coarse)	n_f (fine)	n_c/n_f
8	173*3	735*3	0.24	65*3	537*3	0.12
16	809*3	6975*3	0.12	306*3	4145*3	0.07
24	1951*3	24863*3	0.08	749*3	13897*3	0.05
32	3585*3	60543*3	0.06	1245*3	33729*3	0.04

TABLE 19
The dofs of local problems solved in Step 3 and Step 4 of **Algorithm 4.1**: Maxwell's equations (with Nedelec edge basis functions)

	Ω_{F}			$\Omega_{\mathrm{V}}^{half}$		
d/h	n_c (coarse)	n_f (fine)	n_c/n_f	n_c (coarse)	n_f (fine)	n_c/n_f
8	1673	6240	0.38	1910	5554	0.34
16	6642	53568	0.18	5390	35658	0.15
24	15157	184992	0.08	11076	111842	0.10
32	27132	443520	0.06	16575	255610	0.06

It can be seen from these results that the dofs of local problems in Step 3 and Step 4 of **Algorithm 4.1** are much smaller than that of the local problems associated with the original fine grids. Moreover, the smaller the value d/h is, the better the coarsening effect is. This means that the preconditioner B_{II} is very cheap.

Finally, we illustrate why this coarsening technique has not been applied directly to the preconditioner B_I (see **Remark 4.2**).

In Table 20, we list the dofs of the problems in Step 3 of **Algorithm 3.1**, which associated with the fine partition and the coarsening partition on $\Omega_{\mathrm{V}}^{half}$, respectively.

TABLE 20
The dofs of the local problems solved in Step 3 of **Algorithm 3.1**: coarsening or not

	Elasticity problems			Maxwell's problems		
d/h	n_c (coarse)	n_f (fine)	n_c/n_f	n_c (coarse)	n_f (fine)	n_c/n_f
8	289*3	792*3	0.40	3048	6130	0.50
16	1591*3	4913*3	0.32	14704	37962	0.39
24	3964*3	15625*3	0.25	32115	117026	0.27
32	7256*3	35937*3	0.20	60118	264826	0.23

From Table 20, we can see that the coarsening effect is not ideal for this situation.

7. Conclusion

In this paper, we have constructed two substructuring preconditioners with the simplest coarse space for general elliptic-type problems in three dimensions. In particular, we design two kinds of new local interface solvers, which are easy to implement and do not depend on the considered models. The proposed preconditioners can absorb some advantages of the non-overlapping DDMs and the overlapping DDMs. Especially, in the second preconditioner we propose a coarsening technique to solve local interface problems. As expected, the utilization of coarsen grids can significantly decrease the cost of calculation, but does not destroy the convergence rate of the PCG method. We have given some numerical results to show that the proposed preconditionners are effective uniformly for the linear elasticity problem and Maxwell's equations in three dimensions.

References

[1] J. Bramble, J. Pasciak and A. Schatz, The construction of preconditioners for elliptic problems by substructuring, IV. Math. Comp., 53(1989), pp.1-24.

[2] S. Brenner and L. Sung, BDDC and FETI-DP without matrices or vectors, Comput. Methods Appl. Mech. Engrg., 196(2007), 1429-1435.

[3] X. Cai, An additive Schwarz algorithms for parabolic convection-diffusion equation, Numer. Math., 60(1991), No.1, pp.41-61

[4] X. Cai, The use of pointwise interpolation in domain decomposition methods with nonnested meshes, SIAM J. Sci. Comput., 16(1995), pp. 250-256.

[5] X. Cai and M. Sarkis, A Restricted additive Schwarz preconditioner for general sparse linear system, SIAM J. Sci. Comput., 21(1999), No. 2, pp. 792-797

[6] M. Cessenat. Mathematical methods in electromagnetism. World Scientific, River Edge, NJ, 1998.

[7] T. Chan and J. Zou, Additive Schwarz domain decomposition methods for elliptic problems on unstructured meshes, Numer. Algorithms, 8(1994), pp. 329-346.

[8] T. Chan, B. Smith, and J. Zou. Overlapping Schwarz methods on unstructured meshes using non-matching coarse grids. Numer. Math., 73(2):149-167, 1996.

[9] X. Chen and Q. Hu, Inexact solvers for saddle-point system arising from domain decomposition of linear elatcity problems in three dimensions. Inter. J. Numer. Anal. & Modl., 8(2011), No. 1, p156-173.

[10] E. Chung, H. Kim, and O. Widlund. Two-Level Overlapping Schwarz Algorithms for a Staggered Discontinuous Galerkin Method, SIAM J. Numer. Anal. 51(2013), No.1, 47-67.

[11] C. Dohrmann, A preconditioner for substructuring based on constrained energy minimization, SIAM J,Sci. Comput. vol.25, No. 1, pp. 246-258, 2003.

[12] C. Dohrmann and O. Widlund, An Iterative Substructuring Algorithm for Two-Dimensional Problems in H(curl), SIAM J. Numer. Anal. 50(2012), No.3, pp.1004-1028.

[13] C. Dohrmann and O. Widlund, A BDDC Algorithm with Deluxe Scaling for Three-Dimensional H(curl) Problems, Comm. Pure Appl. Math., 2015, doi: 10.1002/cpa.21574

[14] M. Dryja, J. Galvis, and M. Sarkis, BDDC methods for discontinuous Galerkin discretization of elliptic problems, J. Complexity, 23(2007), 715-739.

[15] M. Dryja, F. Smith and O. Widlund, Schwarz analysis of iterative substructuring algorithms for elliptic problems in three dimensions, SIAM J. Numer. Anal. 31(1994), No.6, pp.1662-1694

[16] M. Dryja, O. B. Widlund, Domain decomposition algorithms with small overlap, SIAM J. Sci. Comput., 15(1994), pp. 604-620.

[17] M. Dryja and O. Widlund, Schwarz methods of Neumann-Neumann type for three- dimensional elliptic finite element problems, Comm. Pure Appl. Math., 48 (1995), pp. 121-155.

[18] O. Dubois and M. Gander, Optimized Schwarz methods for a diffusion problem with discontinuous coefficient, to appear in Numerical Algorithms

[19] C. Farhat and F. Roux, A method of finite element tearing and interconnecting and its parallel solution algorithm, Internat. J. Numer. Methods Engrg., 32 (1991), pp. 1205-1227.

[20] C. Farhat, M. Lesoinne, and K. Pierson, A scalable dual-primal domain decomposition method, Numer. Linear Algebra Appl., 7 (2000), pp. 687-714.

[21] C. Farhat, J. Mandel, and F. Roux, Optimal convergence properties of the FETI domain decomposition method, Comput. Methods. Appl. Mech. Engrg., 115 (1994), pp. 365-388

[22] A. Frommer and D. Szyld, An algebraic convergence theory for restricted additive Schwarz methods using weighted max norms, SIAM J. Numer. Anal., 39 (2001), pp. 463-479.

[23] M. Gander, Optimized Schwarz Methods, SIAM J. Numer. Anal., 44(2006), No. 2, pp. 699-731

[24] M. Gander and F. Kwok, Best Robin parameters for optimized Schwarz methods at cross points, SIAM J. Sci. Comput., 34 (2012), pp. 1849-1879.

[25] C. Geuzaine and J.-F. Remacle, Gmsh: a three-dimensional finite element mesh generator with built-in pre- and post-processing facilities.

[26] G. Haase, U. Langer and A. Meyer, The approximate Dirichlet Domain Decomposition method. Part II: Applications to 2nd-order Elliptic B.V.P.s. Computing 47(2): 153-167 (1991)

[27] R. Hiptmair. Finite elements in computational electromagnetism. Acta Numerica, 11:237-339, 2002.

[28] Q. Hu, Z. Shi and D. Yu, Efficient solvers for saddle-point problems arising from domain decompositions with Lagrange multipliers, SIAM J. Numer. Anal., 42(2004), no. 3, 905-933.

[29] Q. Hu, A Regularized Domain Decomposition Method with Lagrange Multiplier, Adv Comput Math, Vol. 26, No. 4. (May 2007), pp. 367-401

[30] Q. Hu, S. Shu And J. Wang, Nonoverlapping domain decomposition methods with a simple coarse space for elliptic problems. Math.Comput., 79(2010), No.272, pp.2059-2078

[31] Q. Hu, S. Shu and J. Zou. A substructuring preconditioner of three-dimensional Maxwell's equations, Proceedings of the Twentieth International Conference on Domain Decomposition Methods (No. 91 in Lecture Notes in Computational Science and Engineering), pages 73-84, edited by R. Bank, M. Holst, O. Widlund and J. Xu, Heidelberg-Berlin, 2013.

[32] Q. Hu and J. Zou. A nonoverlapping domain decomposition method for Maxwells equations in three dimensions. SIAM J. Numer. Anal., 41(5):1682C1708, 2003.

[33] Q. Hu and J. Zou. Substructuring preconditioners for saddle-point problems arising from Maxwells equations in three dimensions. Math. Comp., 73(245):35-61 (electronic), 2004.

[34] A. Klawonn, O. Widlund and M. Dryja, Dual-Primal FETI methods for three-dimensional elliptic problems with Heterogeneous coefficients. SIAM J. Numer. Anal., 40(2002), 159-179.

[35] H. Kim and X. Tu, A three-level BDDC algorithm for mortar discretizations, SIAM J. Numer. Anal., 47(2009), 1576-1600.

[36] J. Li and O. Widlund, On the use of inexact subdomain solvers for BDDC algorithms, Comput. Methods Appl. Mech. Engrg., 196(2007), 1415-1428.

[37] J. Mandel and M. Brezina, Balancing domain decomposition for problems with large jumps in coefficients, Math. Comput., 65 (1996), pp. 1387-1401.

[38] J. Mandel and C. Dohrmann, Convergence of a balancing domain decomposition by constraints and energy minimization, Numer. Linear Algebra Appl., 2003.

[39] J. Mandel, C. Dohrmann and R. Tezaur. An algebraic theory for primal and dual substructuring methods by constraints. Appl. Numer. Math., 54(2005), 167-193.

[40] P. Monk. Finite Element Methods for Maxwells Equations. Oxford University Press, Oxford, 2003.

[41] B. Smith. An optimal domain decomposition preconditioner for the finite element solution of linear elasticity problems. SIAM Journal on Scientific and Statistical Computing, 13(1992), No.1, pp.364-378.

[42] A. Toselli. Overlapping Schwarz methods for Maxwells equations in three dimensions. Numer. Math., 86:733C752, 2000.

[43] A. Toselli. Dual-primal FETI algorithms for edge finite element approximations in 3D. IMA J. Numer. Anal., 26:96C130, 2006.

[44] A. Toselli, O. Widlund. Domain decomposition methods: algorithms and theory. Berlin: Springer, 2005.

[45] L. Veiga, D. Cho, L. Pavarino, S. Scacchi, Overlapping Schwarz methods for Isogeometric Analysis, SIAM J. Numer. Anal., 50(2012), 1394-1416.

[46] L. Veiga, L. Pavarino, S. Scacchi, O. Widlund and S. Zampini, Isogeometric BDDC Preconditioners with Deluxe Scaling, SIAM J. Sci. Comput., 36(2014), No. 3, pp. 1118-1139

[47] J. Xu and Y. Zhu, Uniform convergent multigrid methods for elliptic problems with strongly discontinuous coefficients, M3AS, 18(2008), 77-105.

[48] J. Xu and J. Zou, *Some non-overlapping domain decomposition methods*, SIAM Review, 40(1998), 857-914